



Contents lists available at ScienceDirect

Arabian Journal of Chemistry

journal homepage: www.ksu.edu.sa

Natural deep eutectic solvent-ultrasound for the extraction of flavonoids from *Fructus aurantii*: Theoretical screening, experimental and mechanism

Hua Du^{a,1}, Wenhui Wu^{a,1}, Yaodeng Wang^{a,b}, Ping Tang^a, Yi Wu^a, Jing Qiu^a, Chong Xu^a, Lingzi Li^b, Min Yang^{a,*}

^a Department of Preparation Center, Chongqing Hospital of Traditional Chinese Medicine, Chongqing 400014, China

^b College of Pharmacy, Chengdu University of TCM, Sichuan 611137, China

ARTICLE INFO

Keywords:

NADES

Flavonoids

Fructus aurantii

COSMO-RS

DFT

Extraction mechanism

ABSTRACT

To reduce the environmental pollution caused by organic solvents and improve the extraction efficiency, a green and high-effective natural deep eutectic solvent (NADES) was screened out and prepared for the extraction of flavonoids from *Fructus aurantii* based on the COMOS-RS and experimental verification. The results showed the results of theoretical screening and experimental verification were consistent, and Ch-Lea was the best extraction solvent, which further proved the COMOS-RS was an efficient tool for the solvent screening. Then, the extraction conditions were investigated. The optimum extraction conditions were as follows: molar ratio (1:2), water content (30%), solid-liquid ratio (1/60 g/g) and extraction time (15 min), yet the extraction temperature and power did not significantly affect the extraction yield. Under the optimal extraction condition, the extraction yield of flavonoids was 122.68 mg/g. Compared with the traditional extraction solvents (methanol and ethanol), Ch-Lea has a higher extraction yield. And the green assessment was conducted based on Eco-Scale methodology, which results indicated the Ch-Lea was more environmentally friendly than methanol and ethanol. Meanwhile, the Ch-Lea has good reusability, and the extraction yields from four reuses were 122.68 mg/g, 125.13 mg/g, 122.56 mg/g and 105.63 mg/g, respectively. Moreover, the extraction mechanism was delved into using molecular dynamics (MD) simulation and reduced density gradient (RDG) analysis. The hydrogen bond interaction, particularly the O-H bonds, between Ch-Lea and the naringin molecule emerged as the primary force driving the extraction process. In summary, Ch-Lea is a green, economical, and highly effective solvent, making it a promising candidate for flavonoid extraction from *Fructus aurantii*. Its potential as an alternative to traditional extraction solvents further underscores its value.

1. Introduction

Fructus aurantii, known as Zhi qiao in Chinese, is the dried mature fruit of *Citrus aurantium* L. and is a traditional herb widely used in China for thousands of years, with diverse pharmacological effects (Yang et al., 2020). A large number of clinical observations and practices have proved its clinical efficacy. It was usually employed to treat diabetes, kidney stones and a variety of cancers, depression, cardiovascular diseases, gastrointestinal diseases, etc (Li et al., 2015; Zhang et al., 2012). The chemical components of *Fructus aurantii* mainly contain flavonoids, volatile oils and alkaloids. Among them, the flavonoids play a major role in pharmacological efficacy. Such as the flavonoids had a certain hepatoprotective effect, and its mechanism may be that hesperidin can

inhibit hepatocyte apoptosis and reduce the activity of COX-2 in liver tissue (Pari et al., 2011). Naringin, a flavonoid component, possesses notable anticancer properties, specifically exhibiting its efficacy in inducing apoptosis in human hepatocellular carcinoma HepG2 cells. This apoptotic effect is mediated through the activation of mitochondrial-dependent caspase-9 and the caspase-8-induced hydrolysis of Bid protein, thereby demonstrating its potential as a therapeutic agent against cancer (Banjerdpongchai, et al., 2016).

Due to the potential benefits and medicinal value of the flavonoids in *Fructus aurantii*, a large number of studies have been carried out to maximize its extraction efficiency (He et al., 2018). However, the extraction solvents used in these studies were all organic solvents, including methanol, ethanol, acetone, chloroform, etc (He et al., 2018).

* Corresponding author.

E-mail address: cqyangmin@126.com (M. Yang).

¹ Hua Du and Wenhui Wu contributed equally to this work.

It is widely known that organic solvents have a number of disadvantages, including inflammable, explosive, toxic, polluting the environment, and may even leave unacceptable residues in the extract, which limits the sustainability of the extraction process (Cui et al., 2021). Therefore, it is urgent to seek a green and efficient alternative solvent for extracting flavonoids from *Fructus aurantii*.

Natural deep eutectic solvent (NADES), as a kind of emerging green solvent, is encouraged as a potential alternative for traditional organic solvents (Mushtaq et al., 2022; Wang, et al., 2021). NADES consists of a hydrogen bond donor (HBD) and a hydrogen bond acceptor (HBA) through hydrogen bond interactions (Noormohammadi et al., 2022; Yang et al., 2023a). The HBD and HBA are primarily composed of natural components that are present in cells and organisms, such as organic bases, amino acids, sugars, choline derivatives and food additive, and thus the NADES has characteristics such as biodegradability, non-toxicity or acceptable pharmacological toxicity profiles, which have been favorably received by the scientific community (AlYammahi et al., 2023; Dai et al., 2013; Zannou et al., 2020). Compared to the composition of NADES (HBD or HBA), NADES has a remarkable low melting point and unique physicochemical characteristics, thus NADES possess several valuable properties including negligible volatility, high solvating ability, sustainability and stability (Alañón et al., 2020; Della et al., 2022; Nian et al., 2022). Therefore, NADES has been widely used in the extraction of chemical components in various plants (Cheng et al., 2024; Khajavian et al., 2022; Zannou et al., 2022; Zuo et al., 2023). For example, Hsieh et al. synthesized several alcohol-based DESs by the ultrasonication-assisted method, and it was combined with the ultrasonic-assisted extraction method for the extraction of gingerol from ginger powder (Hsieh et al., 2020). The results showed that the extraction performance of the prepared DESs was significantly better than that of traditional organic solvents. Pan et al. prepared a novel three-component natural eutectic solvent (3c-NADES) with betaine, triethanolamine and $MgCl_2 \cdot 6H_2O$ as raw materials, and successfully extracted three main active substances from *Acanthopanax* stems based on microwave ultrasonic-assisted technology (Pan et al., 2021). Yang et al. tailored several NADES, of which choline chloride-oxalic acid (ChCl-Oa) was the most effective for ellagic acid extraction from *Geum japonicum*. Under optimal conditions, ChCl-Oa has a higher extraction yield than common organic solvents including methanol, ethanol and acetone (Yang et al., 2023b). In conclusion, NADES can be used as a green and efficient extraction solvent for the extraction of flavonoids from *Fructus aurantii*.

Meanwhile, NADES has the characteristics of tailor-made, which can design different combinations of HBD and HBA according to the physical and chemical properties of the target compound (Wang et al., 2024a). However, due to there is a lot of types of HBD and HBA, and the number of NADES is equal to the product of the number of HBA and HBD, so a large number of NADES combinations will be generated. Therefore, the trial-and-error method of traversing measurements and the empirical method of selecting the most promising NADES are not feasible, which is time-consuming, labor-intensive and inefficient. Thus, a scientifically valid screening method is needed to predict the solubility and extraction efficiency of NADES for flavonoids.

Recently, the conductor like real solvation screening model (COSMO-RS), a thermal dynamic model based on quantum chemical calculation, has been proposed and utilized as a modeling and prediction tool for liquid equilibrium (Quaid et al., 2023). COSMO-RS has proven to be a powerful tool for predicting the solubility of small molecule compounds and polymers, which can calculate the chemical potential of the small molecule compounds or polymer in a liquid solution, thus predicting the solubility coefficient and activity coefficient (Doldolova et al., 2021; Khan et al., 2023; Mohan et al., 2022). Wang and his co-workers use COSMO-RS to predict the extraction solubility and efficiency of NADES to lentinan from shiitake mushrooms, and it is successfully verified by experiments (Wang et al., 2024b). Zhao et al. calculated the activity coefficient (γ), excess enthalpy (HE) and σ -profile

between hemicellulose and solvent by using the COSM-RS, so as to predict its ability to dissolve hemicellulose (Zhao et al., 2022). Lazović et al. used the COSM-RS tool to pre-screen a large number of natural eutectic solvents for improving the efficiency of phenolic extraction from *Teucrium chamaedrys*, and the experimental results showed that COSM-RS was a suitable method to simulate NADES properties (Lazović et al., 2023). Therefore, COSM-RS can be used to predict the solubility of flavonoids in NADES, and to predict the extraction efficiency of NADES to extract flavonoids from *Fructus aurantii*.

To sum up, the overall purpose of this study is to design and synthesize a green NADES solvent, which could replace the traditional extraction solvent, and to establish a sustainable extraction method of flavonoids from *Fructus aurantii*. The specific objectives were as follows: (i) to design and synthesize suitable NADES based on COMSO-RS tools according to the structural characteristics of the target molecule (eg. naringin). (ii) to optimize the molar ratio and water content of NADES and the extraction conditions, such as extraction temperature, extraction time, extraction power and solid-liquid ratios, so as to improve the extraction efficiency. (iii) to evaluate NADES greenness and safety by Eco-Scale methodology. (iv) to analyze the mechanism of NADES through molecular dynamics, RDG analysis, and SEM analysis.

2. Materials and methods

2.1. Material and chemical reagent

Fructus aurantii sample was collected from the planting base, Jiangjin District, Chongqing. After samples were dried at 60 °C, powdered and sieved using an 80-mesh sieve. Choline chloride (Ch, >98 %), ethylene glycol (Eth, ≥99.5 %), levulinic acid (Lea, ≥99.5 %), citric acid (Cia, ≥99.5 %), urea (Ur, ≥99 %), lactic acid (Laa, ≥99.5 %), tartaric acid (Taa, ≥99.5 %), methanol and ethanol (Analytical grade) were supplied by Aladdin Biochemical Technology (Shanghai, China). Methanol, acetonitrile and phosphoric acid (HPLC-grade) were supplied by Sino-pharm Chemical Reagent (Shanghai, China). The analytical standards of flavonoids, including naringin and neohesperidin, were purchased from the National Institutes for Food and Drug Control (Beijing, China).

2.2. Preparation and characterization of NADES

The preparation of NADES was based on previous reports. Briefly, the HBA and HBD were accurately weighed according to a fixed molar ratio and mixed into 250 mL glass flasks. The mixture is then magnetically stirred in a water bath and heated at 50 °C – 90 °C until a homogeneous, transparent liquid is formed.

The viscosity of NADES was determined using a rheometer (MCR 302, Anton Paar GmbH, Austria), and the measure condition was a constant shear rate of 0.1 s⁻¹ at 25 °C for 10 s. The functional groups characteristics of HBA, HBD and NADES were analyzed by Fourier Transform infrared spectroscopy (Nicolet 6700, Thermo Fisher Scientific, Waltham, MA, USA) by ATR method at room temperature. The spectral range was 4000 – 400 cm⁻¹ and the resolution were 4 cm⁻¹, and the infrared spectra data was recorded by OMIC software. The NMR hydrogen spectrum (H¹ NMR) characteristics was measured by nuclear magnetic resonance (NMR) spectrometer (AVANCE NEO 400, Bruker, Germany).

2.3. Extraction of flavonoids

For the initial screening of the NADES system, an amount of 0.10 g of *Fructus aurantii* sample powder was accurately weighted in 25 mL glass flasks, and mixed with 6 g of NADES. Then, the extraction was performed by an ultrasonic bath (USC 2100 THD, VWR, UK) and with ultrasonic irradiation at 50 °C for 30 min, the frequency and power of the ultrasonic was 40 KHz and 300 W. The suspension was accurately transferred to a 25 mL volumetric flask and diluted with water. The

sample solution was then passed through a 0.45- μm filter membrane for HPLC analysis. When the sample solution passes through the 0.45 μm filter membrane, the middle part of the continuous filtrate was used, and the filtrate of the initial part was discarded. For the single-factor experiment, several important factors are examined for optimizing the extraction conditions, including the mole ratio of HBA and HBD (1:1, 1:2, 1:3, 1:4 and 1:5), water content of NADES (0, 10 %, 20 %, 30 %, 40 %, 50 %, 60 % and 70 %), and solid–liquid ratios (1:20, 1:30, 1:40, 1:60, 1:80 and 1:100 g/g), extraction time (1, 5, 15, 30, 40 and 60 min), extraction temperature (20, 30, 40, 50, 60 and 70 °C) and extraction power (60, 120, 180, 240 and 300 W). Three parallel experiments were performed for each extraction. The extraction yield was calculated by the following equation:

$$Y = \frac{c \times v}{m} \quad (1)$$

where the c (mg/mL) is the concentration of flavonoids, which is the sum of naringin and neohesperidin. The v (mL) is the total volume after dilution. The m (g) is the mass of *Fructus aurantii* sample used in the extraction.

2.4. HPLC analysis

The quantitative analysis of naringin and neohesperidin was carried out by HPLC (1260 Agilent HPLC, Agilent Technologies Co. Ltd, USA), and it equipped with a G7114A 1260 VMD detector and a Phenomenex C₁₈ column (250 mm \times 4.6 mm, 5 μm). The column temperature is 30 °C. The injection volume and flow rate were 10 μL and 1.0 mL/min, respectively. The detection wavelength was 283 nm. The mobile phase was 0.2 % phosphoric acid – water (A) and acetonitrile (B), and the gradient elution procedure was as follows: 0—2 min 90 % A, 2—5 min 90 % \rightarrow 85 % A, 5—10 min 85 % \rightarrow 82 % A, 10—32 min 82 % \rightarrow 80 % A, 32—45 min 80 % \rightarrow 60 % A, 45—60 min 60 % \rightarrow 40 % A, 60—60 min 40 % \rightarrow 0 A (Wang et al., 2024). The HPLC chromatogram was shown in Fig. S1.

2.5. Reusability of NADES

Following the previously refined extraction technique and procedure, a filtration step was performed on the solid–liquid mixture after extraction with fresh Ch-Lea solvent. Subsequently, the filtered Ch-Lea solvent, retaining its flavonoid content, was recycled and reused for extracting a fresh batch of *Fructus aurantii* samples. Subsequently, an analysis was conducted to assess the incremental accumulation of flavonoids in the extract.

2.6. SEM of extraction residue

The morphologies of raw sample powder and the solid residues after extraction by NADES were analyzed with a Thermo Scientific™ APREO SEM (Thermo Fisher Scientific, Waltham, MA, United States). In short, the sample is first mounted on an aluminum stump, then sputtered with a thin layer of gold, and finally observed through the In-lens SE detector of SEM. The drying method of sample was as follows: the sample was quickly put into liquid nitrogen to freeze and solidify the sample, and then the sample was transferred into a vacuum coating instrument and sublimated under high vacuum. The dehydrating agent was directly changed from solid to gas, and the sample was dried.

2.7. Theoretical calculation

Due to the naringin and neohesperidin has similar chemical structures and properties, thus only naringin molecule was used as the target compounds for solvent screening and theoretical calculation. Material Studio (MS) 2020 software was applied to draw the structure of molecules (HBD, HBA, NADES and naringin). NADES consists of HBD and

HBA, and they were combined into one molecule as NADES according to the set molar ratio. And Dmol3 module was then applied to optimize the geometric structure, moreover, the interaction energy between NADES and naringin was calculated. The calculation formula is as following:

$$E_b = E_T - (E_1 + E_2) \quad (2)$$

where the E_b (Kcal/mol) is the binding energy between NADES and naringin. The E_T (Kcal/mol) is the total energy of NADES and naringin. The E_1 (Kcal/mol) and E_2 (Kcal/mol) were the energy of NADES and naringin, respectively.

COSMO-RS simulation and calculation were carried out using the COSMOthermX 19.0.5 software. Since the series of NADES to be studied in this paper are not found in the database of COSMOthermX®, Materials Studio software was used to draw and optimize the molecular geometry of the components, and further calculated through the Dmol3 module of Materials Studio software to obtain the cosmo file required for COSMO-RS calculation. It was applied to calculate the surface charge densities (sigma-profiles) and sigma potentials of NADES and naringin, and the activity coefficient at infinite dilution (γ^∞) of naringin in different NADES. All calculations were performed at 298 K.

The selected NADES was performed by molecular dynamics simulation (MD). It was based on the Forcite module of Materials Studio (MS) software. The naringin was selected as the target compound, and the solvent system had the composition of NADES and water. A box (32.3 Å \times 32.3 Å \times 32.3 Å) was established by Amorphous Cell Calculation for better equilibration. The particle mesh Ewald method was used to calculate the electrostatic interaction, and the cutoff distance was set as 10 Å. The normal volume temperature (NPT) was calculated at 298 K using the Berendsen temperature coupling method. The time steps were set as 1 fs, and the total simulation time was set as 100 ps. The number of steps was set as 100000, and the track data was stored and frame outputted every 100 steps. In all MD simulation processes, the COMPASS force field was applied.

The weak interaction analysis (Reduced density gradient function, RDG) was performed in combination with Avogadro 1.0.3 software, Orca 4.2.1 software, Multiwfn 3.8 software (Lu et al., 2012) and VMD 1.9.3 software.

2.8. Data statistics and analysis

All experiments were set up with three replicates, and the data were presented as mean \pm standard deviation (SD). The data were dealt with by SPSS 27.0 software, and the date plotting was performed using the Origin 2022 software.

3. Results and discussion

Naringin and neohesperidin, as the main components of flavonoids in *Fructus aurantii*, play a key role in the clinical efficacy of *Fructus aurantii*. Naringin and neohesperidin together account for about 80 % of the total flavonoids, and they have become the focus of the research on *Fructus aurantii* (Yu, et al., 2017). Therefore, naringin and neohesperidin were selected as the target extraction objects in this study, and the extraction yield was calculated and evaluated based on the sum of naringin and neohesperidin.

3.1. Design and theoretical screening of NADES

The COSMO-RS model is usually applied to investigate and predict the influence of HBD and HBA structures on the extraction efficiency of target compounds (AlYammahi et al., 2023). Therefore, the COSMO-RS model was used to screen the solvents (18 kinds of NADESs) used for extracting flavonoids (naringin) from *Fructus aurantii* in the present study, and the infinite dilution activity coefficient (γ^∞) was predicted. The value of γ^∞ is a key parameter to evaluate the extraction efficiency.

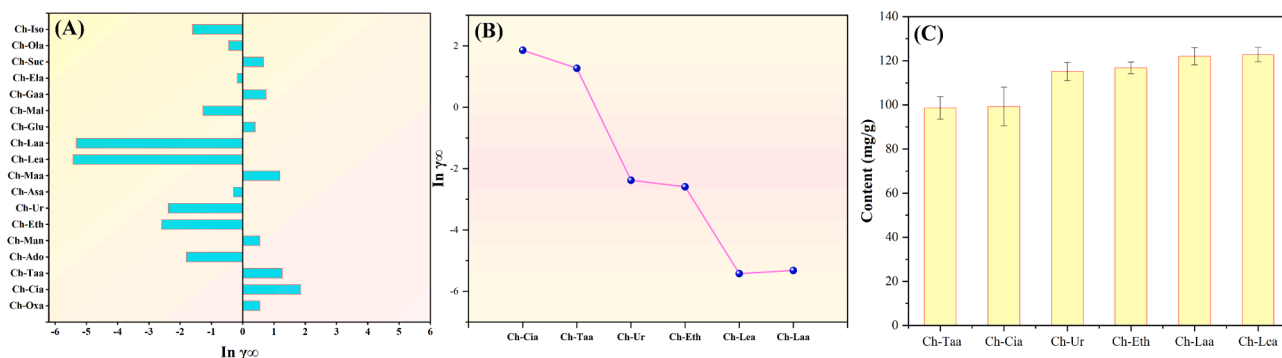


Fig. 1. (A) and (B) the infinite dilution activity coefficient of different NADES and (C) the extraction yield of flavonoids with different NADES.

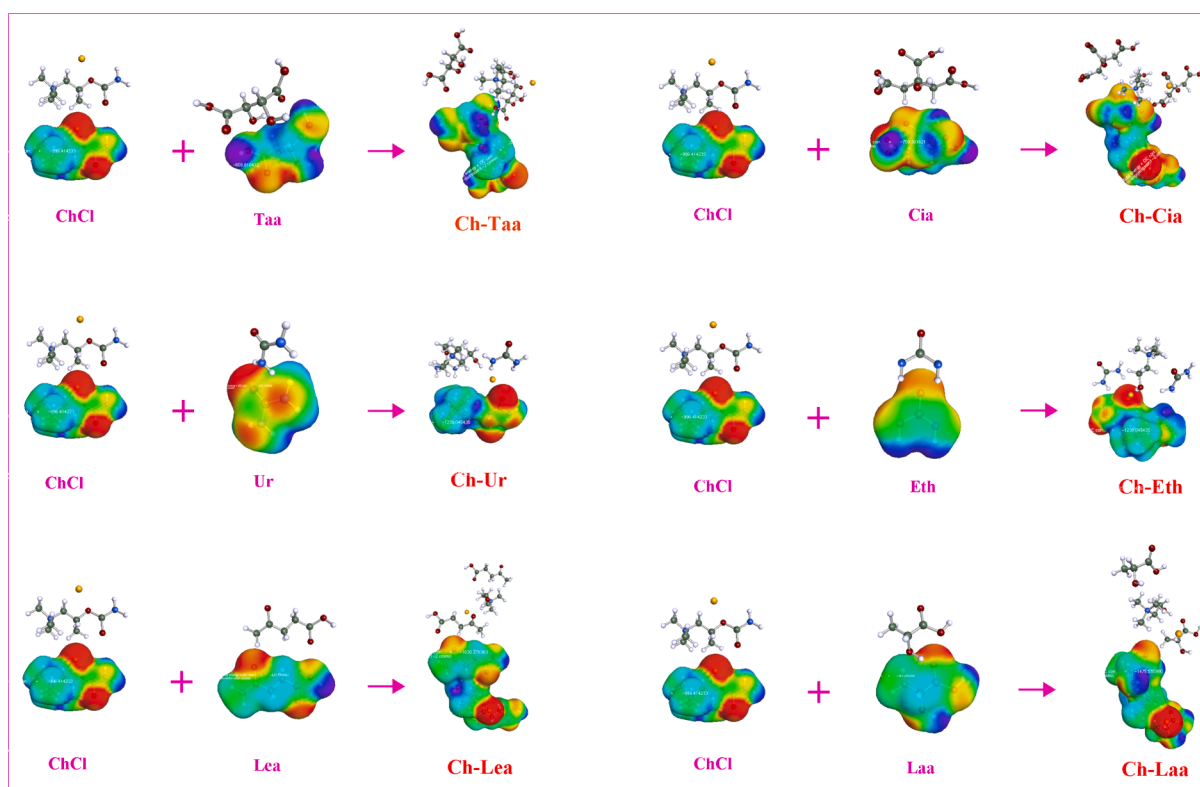


Fig. 2. The molecular structure and charge density of the simulated NADES and their respective components.

The solubility of the target compound in the solvent is inversely proportional to the infinite dilution activity coefficient of the system. A low γ^∞ value indicates that the target compound has a high solubility in the solvent, in other words, the solvent with a low γ^∞ value may have a high extraction efficiency for the compound (Khan et al., 2023). The results of $\ln \gamma^\infty$ value of this study was shown in Fig. 1A. The results showed that the $\ln \gamma^\infty$ value had a significant difference of 18 kinds of NADES, showing the 18 kinds of solvents for the dissolution of naringin ability is different, which further indicated that the extraction efficiency of naringin was significantly different among the 18 NADES solvents. The $\ln \gamma^\infty$ of Ch-Laa (-5.32) and Ch-Lea (-5.42) was significantly smaller than other NADES, and the $\ln \gamma^\infty$ of Ch-Cia (1.86) and Ch-Taa (1.28) was significantly higher than other NADES. The results showed that Ch-Laa and Ch-Lea might have a higher solubility and extraction efficiency for naringin, whereas Ch-Cia and Ch-Taa might have a lower extraction efficiency. In conclusion, according to the predicted results of the COMSO-RS model, Ch-Laa and Ch-Lea were preliminarily considered to be the optimal solvent for naringin extraction.

3.2. Theoretical support of theoretical screening of NADES

In order to understand and explain the principles of theoretical screening at a deeper level, the chemical structure, σ -profile and surface charge density (σ -surface) of the naringin molecule and 6 NADES, which represent high, medium and low $\ln \gamma^\infty$ values, were selected and analyzed by using quantum chemical calculation. The chemical structure and surface charge density (σ -surface) of the naringin molecule and 6 NADES were shown in Fig. 2 and Fig. 3.

3.2.1. σ -surface analysis

The σ -surface is a visual representation of the energy features, and the color of the density cloud surrounding the molecular structure indicates the sigma surface charge (Sellaoui et al., 2017). The blue represents the charge deficit region, the green represents the charge neutral region, and the red represents the charge dense region. The three regions represent the non-polar, mid-polar and polar regions, respectively (Lemaoui et al., 2020). According to Fig. 3A, it could be found that polar

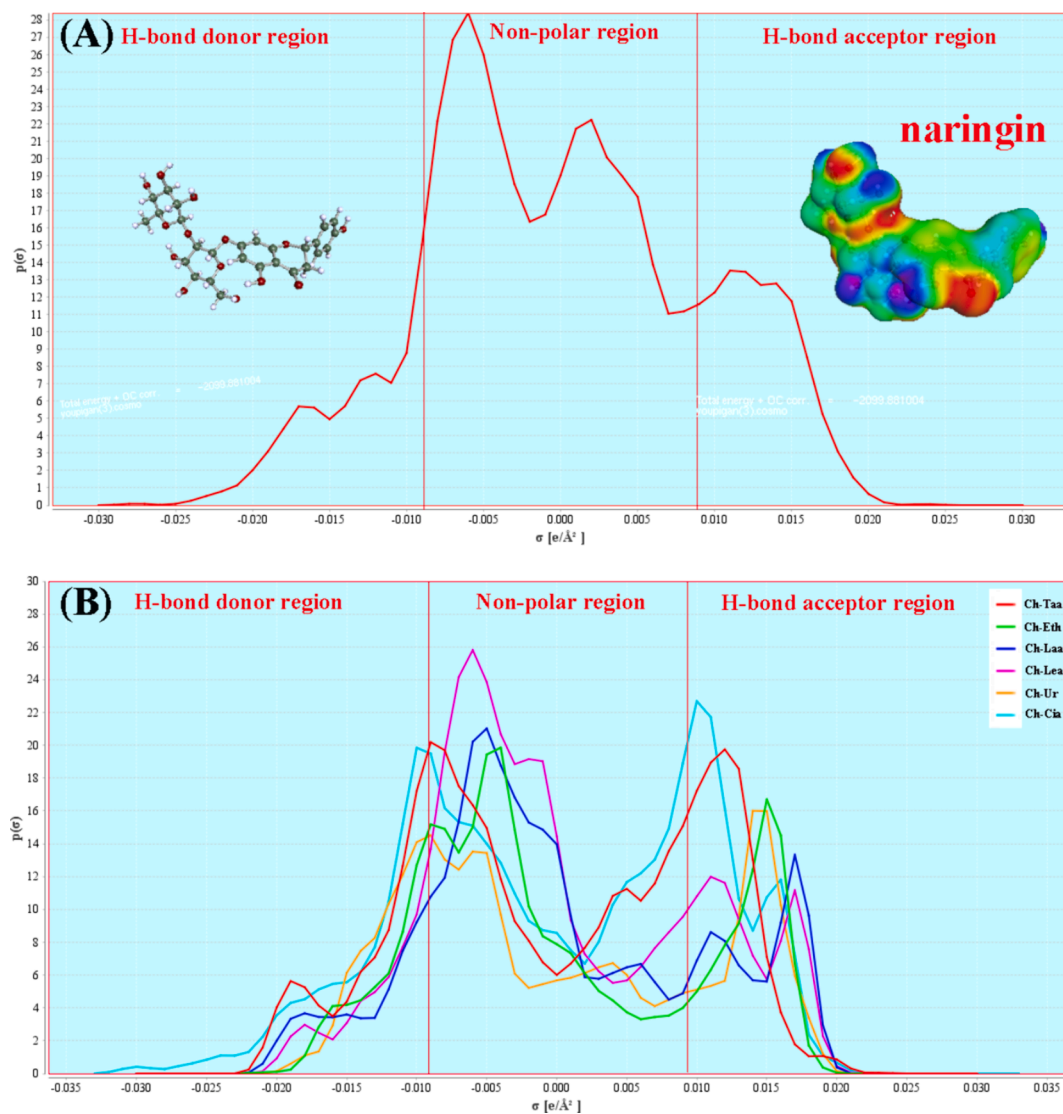


Fig. 3. (A) the σ -profiles of naringin and (B) the σ -profiles of six NADES.

regions of the naringin molecule were mainly attributed to the electron negative difference between the hydrogen (H) and oxygen (O) atoms, leading to the polarization of the hydroxyl group (–OH). And the non-polar regions mainly correspond to a large number of benzene ring structures in the naringin molecule.

The σ -surface could be divided into geometric segments, which are called σ values. The σ -profile is a 2-dimensional compressed histogram of the σ -surface generated in 3D molecular. By analyzing σ -profile plots, sigma values can be evaluated, leading to insight into the intrinsic mechanisms of intermolecular interactions (Quaid et al., 2023).

3.2.2. σ -profile analysis

The σ -profile is generally divided into three regions with $\pm 0.0084 \text{ e}/\text{\AA}^2$ as the threshold. $\sigma < -0.0084 \text{ e}/\text{\AA}^2$ belong to the H-bond donor region (HBD), $\sigma > 0.0084 \text{ e}/\text{\AA}^2$ belong to the H-bond acceptor region (HBA), and $-0.0084 \text{ e}/\text{\AA}^2 < \sigma < 0.0084 \text{ e}/\text{\AA}^2$ belong to the non-polar region (Klamt et al., 2003). The curve containing the area between X-axis values $\pm 0.0084 \text{ e}/\text{\AA}^2$ represents the area that can generate van der Waals interactions with neighboring molecules. The area of curvature above $0.0084 \text{ e}/\text{\AA}^2$ represents the area of the molecular surface available for hydrogen bonding accepting interactions. And the area of curvature less than $-0.0084 \text{ e}/\text{\AA}^2$ indicates the area of the molecular surface available for giving hydrogen bond interactions (Marsh, 2006). The van

der Waals-bond interaction strength is very weak, about an order of magnitude lower than the hydrogen bond interaction energy, so the contribution of the nonpolar region is usually not decisive during NADES formation or extraction and is usually ignored (Sadus, 2019).

From Fig. 3A, it could be found that the σ -profile of the naringin molecule was mainly distributed within the range of $-0.03 \text{ e}/\text{\AA}^2 < \sigma < 0.03 \text{ e}/\text{\AA}^2$. Meanwhile, the curvature area of the H-bond acceptor region (HBA) was greater than the H-bond donor region (HBD), indicating the naringin molecule was more inclined to be an HBA. According to Fig. 3B, it could be observed that the σ -profile of the six NADES were asymmetric and the curvature area of the H-bond acceptor region (HBA) was greater than the H-bond donor region (HBD), the results indicated that these NADES mainly showed HBA potential in the extraction, especially for Ch-Taa and Ch-Cia. The Ch-Taa and Ch-Cia showed strong HBA potential. Due to NADES extracts naringin mainly through the HBA-HBD hydrogen bond interaction, naringin molecule and NADES (Ch-Taa and Ch-Cia) might form competition and repulsion effects of HBA-HBA during the extraction process. Thus, the extraction yield of Ch-Taa and Ch-Cia to naringin was the lowest. Compared with Ch-Taa and Ch-Cia, Ch-Laa and Ch-Lea have smaller HBA potential, so the Ch-Laa and Ch-Lea have less competition and repulsion for the naringin molecule than Ch-Taa and Ch-Cia. Therefore, Ch-Laa and Ch-Lea had higher extraction efficiency than Ch-Taa and Ch-Cia for the extraction of

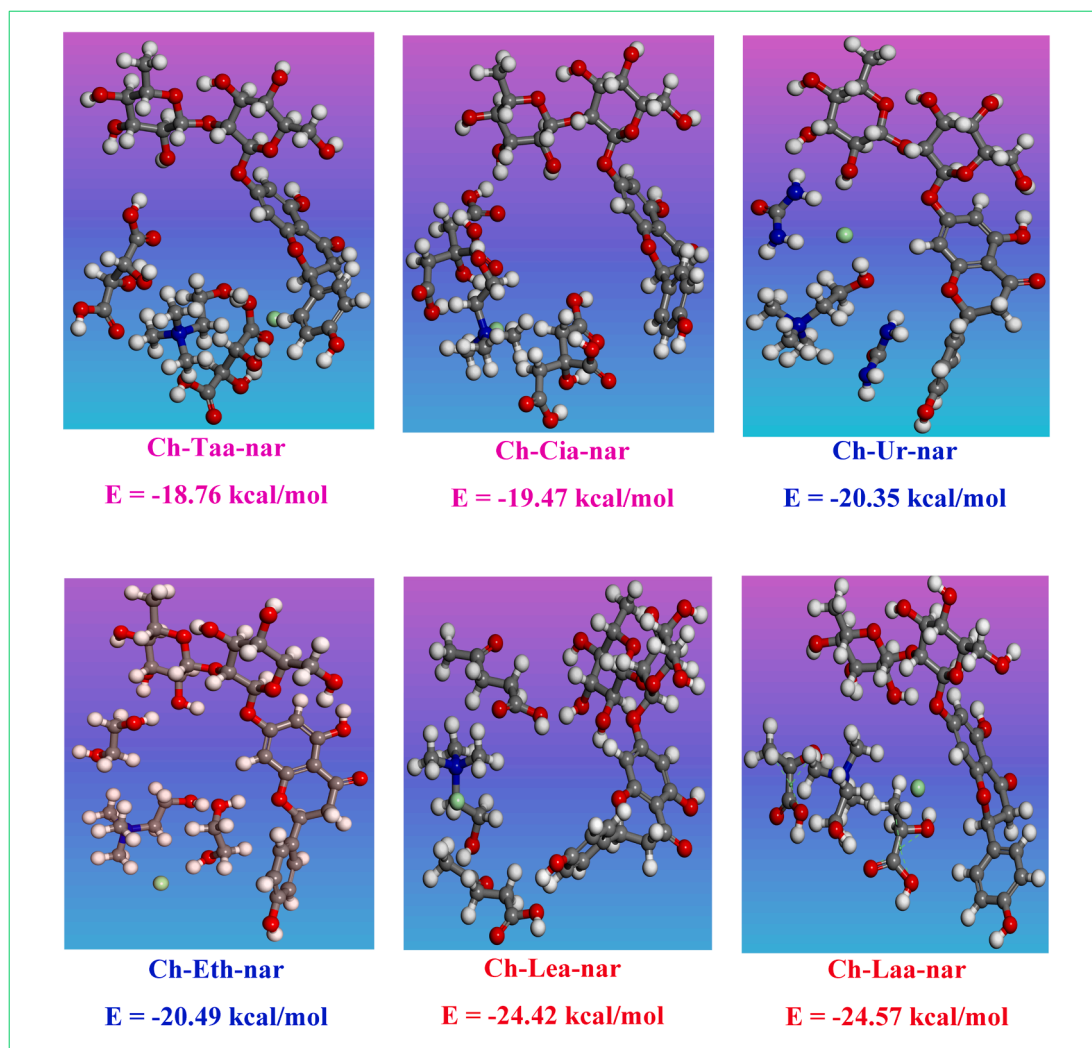


Fig. 4. The binding energy of NADES and naringin.

naringin.

In addition, the peak heights of the σ -profiles can represent the statistical number of surface fragments of molecules with similar polarity. According to the principle of “like dissolves like”, the more similar surface fragments, the better the solubility, and the better the extraction effect (Chang et al., 2020). From Fig. 3A, it could be found the naringin molecule contains a large number of polar and non-polar fragments, and this was consistent with its weak polarity property ($\log P = -0.18$). By comparing the σ -profiles plots of naringin molecule and six NADESs (Fig. 3A and B), it could be found that Ch-Laa and Ch-Lea were more similar to naringin molecule than Ch-Taa and Ch-Cia, indicating that the solubility of naringin and Ch-Laa and Ch-Lea is higher, so Ch-Laa and Ch-Lea has a better extraction ability for naringin.

3.2.3. Binding energy analysis

On the other hand, the binding energies (E_b) between the naringin molecule and the six NADES were calculated. Binding energy can reflect the interaction strength of solvent molecules and solute molecules in solution, thereby indirectly reflecting the solvent's extraction ability towards the target solute (Cheng et al., 2024). The result was shown in Fig. 4, the binding energies between the naringin molecule and Ch-Laa and Ch-Lea were -24.57 kcal/mol and -24.42 kcal/mol, respectively, while that between Ch-Taa and Ch-Cia and naringin molecule was only about -18.76 kcal/mol and -19.47 kcal/mol, respectively. These implied the stronger interaction between the Ch-Laa and Ch-Lea and

naringin molecule than Ch-Taa and Ch-Cia. It was consistent with the conclusion of the previous analysis of σ -profiles.

To sum up, the σ -profiles and binding energies analysis greatly supported the inferences of infinite dilution activity coefficient (γ^∞) in Fig. 1A. Therefore, Ch-Laa and Ch-Lea were considered the best solvent for extracting flavonoids from *Fructus aurantii*. Meanwhile, in order to simplify the research, the study chose Ch-Lea for further extraction experiments, process optimization, structural characterization and mechanism analysis.

3.3. Correlation between theoretical prediction and experimental result

To further verify the reliability of the theoretical calculation results, the extraction experiment of flavonoids of *Fructus aurantii* was performed. For the sake of a simple and brief illustration, only six NADESs, which represent high, medium and low $\ln\gamma^\infty$ values, were selected for preparation and extraction experiments. The six NADESs include Ch-Laa and Ch-Lea (high $\ln\gamma^\infty$ value group), Ch-Ur and Ch-Eth (medium $\ln\gamma^\infty$ value group), as well as Ch-Taa and Ch-Cia (low $\ln\gamma^\infty$ value group) (Fig. 1B). The extraction yield of six NADESs were shown in Fig. 1C. According to Fig. 1C, it could be observed that experimental results were consistent with the theoretical calculations, that is, the extraction yield of Ch-Laa and Ch-Lea in the high $\ln\gamma^\infty$ value group was the highest, and that of Ch-Taa and Ch-Cia in the low $\ln\gamma^\infty$ value group was the lowest. The results were consistent with those of previous reports (Cui et al.,

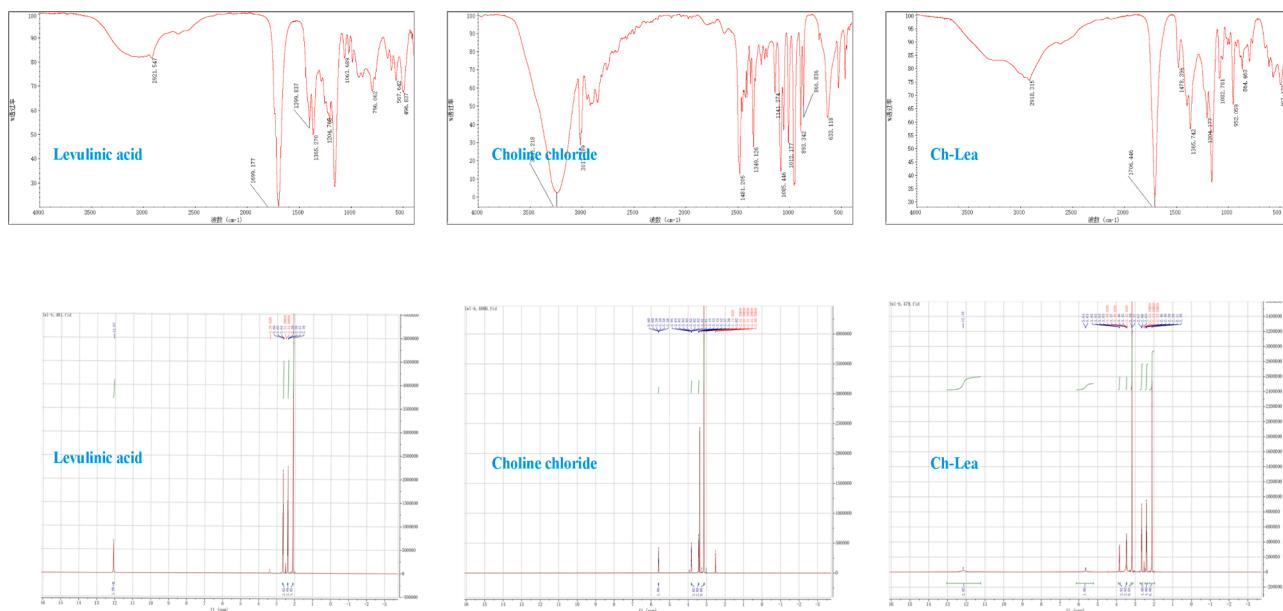


Fig. 5. The FTIR spectrum and ^1H NMR spectrum of Ch-Lea.

2021; Hu et al., 2023). Therefore, it could be concluded that the theoretical calculation was reliable.

3.4. Characterization of NADES

In order to further investigate the composition and properties of NADES (Ch-Lea), FTIR and ^1H NMR analysis was conducted. The IR spectra of choline chloride, levulinic acid and NADES (Ch-Lea) were shown in Fig. 5. It could be observed that there is no significant increase or decrease in the functional groups of NADES (Ch-Lea), compared to the choline chloride and levulinic acid, which indicated that no chemical

changes occurred during the synthesis process of Ch-Lea. In the IR spectra of levulinic acid, the bands located at 1699.177 cm^{-1} and 2921.547 cm^{-1} correspond to the stretching vibrations of the $\text{C}=\text{O}$ and $\text{C}-\text{H}$ groups. In the IR spectra of choline chloride, the bands located at 3017.399 cm^{-1} and 1481.205 cm^{-1} correspond to the stretching vibrations of the $\text{C}-\text{H}$ and $\text{C}-\text{N}$ group. The absorption peak around 3000 cm^{-1} corresponds to $\text{O}-\text{H}$ on Choline chloride and levulinic acid. Interestingly, in the IR spectra of Ch-Lea, the absorption peak of $\text{O}-\text{H}$ extends from 2500 to 3700, and the position of the absorption peak has also undergone a slight shift, which might be due to strong hydrogen bonding in the solvent (Jangir et al., 2020).

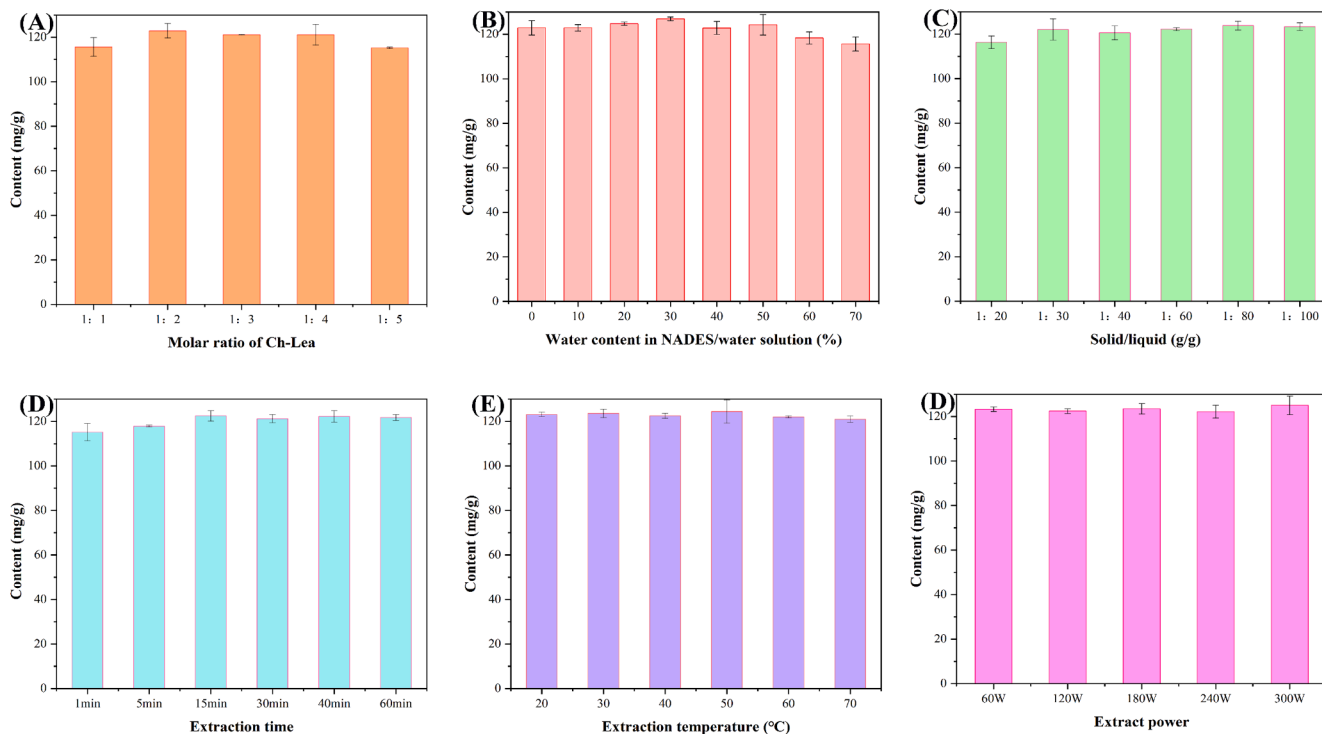


Fig. 6. (A) The extraction content of flavonoids with Ch-Lea. (A) The effect of the molar ratio of Ch-Lea, (B) water content in NADES/water solution, (C) solid/liquid, (D) extraction time, (E) extraction temperature, (F) extraction power.

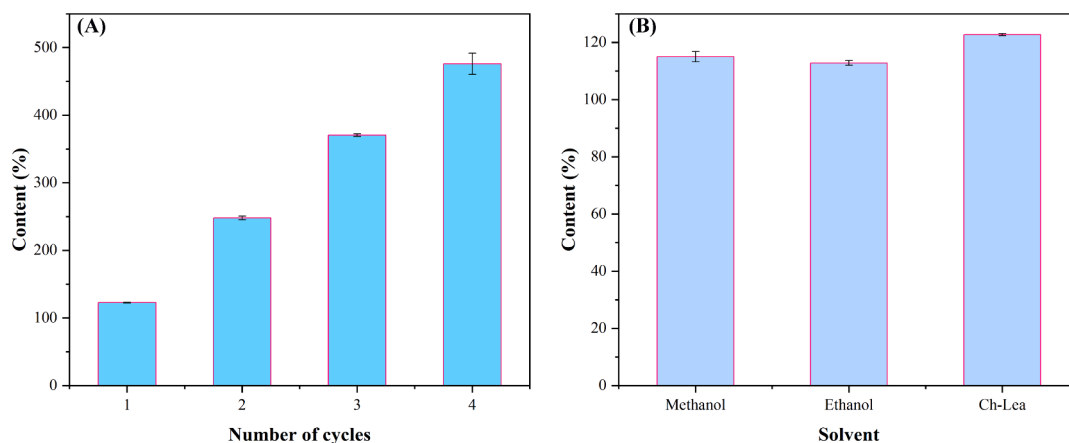


Fig. 7. (A) The extraction rate of four repeated uses of Ch-Lea. (B) The extraction rate of methanol, ethanol and Ch-Lea.

The ^1H NMR spectra of choline chloride, levulinic acid and Ch-Lea were shown in Fig. 5. The choline chloride has four characteristic peaks [$\delta = 5.6$ ppm (1H), $\delta = 3.8$ ppm (2H), $\delta = 3.4$ ppm (2H), $\delta = 3.1$ ppm (9H)]. The levulinic acid has four characteristic peaks [$\delta = 12.1$ ppm (1H), $\delta = 2.6$ ppm (2H), $\delta = 2.4$ ppm (2H), $\delta = 2.1$ ppm (3H)]. The Ch-Lea (molar ratio = 1:2) has eight characteristic peaks [$\delta = 12.1$ ppm (2H), $\delta = 5.6$ ppm (1H), $\delta = 3.8$ ppm (2H), $\delta = 3.4$ ppm (2H), $\delta = 3.1$ ppm (9H), $\delta = 2.6$ ppm (4H), $\delta = 4.4$ ppm (4H), $\delta = 2.1$ ppm (6H)]. The above results showed that the chemical shift (δ) and number of H atoms of Ch-Lea were the same as those of choline chloride and levulinic acid, which further proved that Ch-Lea did not undergo any chemical reaction during the preparation process, indicating that Ch-Lea was a mixture of multiple components coexisting.

3.5. Screening extraction conditions

The molar ratio of HBA-HBD is an important factor affecting extraction efficiency, which may affect hydrogen bonding interactions. The effect of the molar ratio of HBA (Ch) and HBD (Lea) on the extraction yield of flavonoids was shown in Fig. 6A and Table S1-S6. It could be found that the extraction yield of flavonoids reached the maximum value when the molar ratio of Ch to Lea was 1:2. Therefore, a molar ratio of 1:2 between Ch and Lea was most appropriate. The reason for the poor extraction of NADES (Ch to Lea 1:1) may be due to its high viscosity. And the decrease in extraction efficiency with increasing molar ratio may be because the properties of NADES are more similar to Lea as the molar ratio increases.

NADES usually has a high viscosity, which reduces the ability of the solvent to diffuse and penetrate, and this is not conducive to the extraction process. Therefore, a certain amount of water is usually added to improve the viscosity and fluidity of NADES. However, too much water could break the hydrogen bonds of NADES, resulting in a decrease in the stability of NADES. In conclusion, choosing the appropriate water content is very important for the stability and extraction yield of NADES. In the current study, the effect of the water content in NADES on the extraction yield was shown in Fig. 6B. It could be found that the extraction yield of flavonoids showed a tendency to increase (from 0 to 30 %) and then decrease (from 40 % to 70 %) as the percentage of water increases. And the maximum extraction yield was achieved at a water content of 30 %. Therefore, a water content of 30 % in Ch-Lea was optimal for flavonoid extraction. The effect of the ratio of solid/liquid on the extraction yield was shown in Fig. 6C. From the figure, it can be found that the extraction yield of flavonoids is positively correlated with the solid/liquid ratio. When the solid/liquid ratio was higher than 1:60, the increase in extraction yield slowed down, therefore, the solid/liquid ratio of 1:60 was selected as the optimal ratio in this study. As is shown in Fig. 6D, the influence of extraction time on extraction yield was

investigated. It could be observed that the extraction amount reaches 115.14 mg/g when the extraction time is 1 min, and the extraction yield reaches its maximum value at 15 min, indicating that Ch-Lea could quickly extract flavonoids from *Fructus aurantii*. The effect of extraction temperature and extraction power on the extraction yield was shown in Fig. 6E-F. The result showed the extraction temperature and extraction power did not have a significant effect on extraction yield. It is worth noting that the extraction temperature should not be too high, as a high extraction solution temperature may lead to the decomposition of the target component, thereby reducing the extraction yield. This study selected extraction temperature and power of 30 °C and 300 W, respectively.

According to reports by Radošević et al., the excessive acidity of DES may alter the pH value of the cell growth environment, thereby affecting cell viability (Radošević et al., 2016). Therefore, in order to reduce the impact of its acidity on cells, this study adjusted the pH value of Ch-Lea from 1.45 to pH = 5 by adding an appropriate amount of NaOH. At the same time, the extraction ability of flavonoids from *Fructus aurantii* with different pH values of Ch-Lea as extraction solvent was compared. The results showed that there was no significant difference in the extraction yield of Ch-Lea with different pH values, indicating that pH had no significant effect on the extraction yield for flavonoids (Fig. S2).

3.6. Reusability of NADES

To examine the cost-effectiveness and sustainability of Ch-Lea, its reusability was analyzed. The results were shown in Fig. 7A. The results showed that the extraction yield of flavonoids was almost consistent in the first three repeated extractions, with a slight decrease in the fourth repeated extraction. The extraction yields were 122.68 mg/g, 125.13 mg/g, 122.56 mg/g and 105.63 mg/g, respectively. It indicated that Ch-Lea had good reusability.

3.7. Comprehensive evaluation of NADES as green extract solvent

3.7.1. Comparison between NADES and conventional extraction solvents

In order to further understand the advantages of NADES (Ch-Lea), the extraction yields of Ch Lea were compared with the reported traditional extraction solvents (50 % methanol and 20 % ethanol). As shown in Fig. 7B, the flavonoid extraction yield of Ch-Lea, methanol (50 %) and ethanol (20 %) were 122.68 mg/g, 115.01 mg/g and 112.81 mg/g, respectively. The results showed that the extraction yields of NADES (Ch-Lea) were higher than those of methanol and ethanol, indicating that NADES (Ch-Lea) is a high-efficiency extraction solvent.

3.7.2. Green assessment using Eco-Scale methodology

In order to evaluate and compare the greenness of the extraction

Table 1

Eco-Scale-score assessment for the methanol extraction, ethanol extraction and Ch-Lea extraction.

Methanol extraction		Ethanol extraction		Ch-Lea extraction	
Reagents	PPs	Reagents	PPs	Reagents	PPs
Methanol	12.35	Ethanol	1.39	Ch-Lea	0.98
Instruments	PPs	Instruments	PPs	Instruments	PPs
Ultrasound power (<1.5KWh per extraction)	1	Ultrasound power (<1.5KWh per extraction)	1	Ultrasound power (<1.5KWh per extraction)	1
Occupational hazard	3	Occupational hazard	3	Occupational hazard	0
Waste	3	Waste	3	Waste	1
Total PPs	19.35	Total PPs	8.39	Total PPs	2.98
Eco-Scale-score	80.65	Eco-Scale-score	91.61	Eco-Scale-score	97.02

method in this study with traditional extraction methods, the Eco-Scale methodology was applied (Gatuszka et al., 2012; Yang et al., 2023). The calculation method for the score on the Eco-Scale was as follows:

$$E_{score} = 100 - PPs_{reagents} - PPs_{instruments}$$

$$PPs_{reagents} = (I_p + I_s) \times 0.1C \times a$$

where the E_{score} represents the total score of the Eco-Scale; the $PPs_{reagents}$

represents the penalty score for the reagent; the $PPs_{instruments}$ represents the penalty score for the instruments; the I_p represents the number of pictograms for each solvent; the I_s represents the number of signal word (“danger = 2” and “warning = 1”) for each solvent; the C represents the molar concentration for each solvent (mol/L); the a represents the volume constant ($V < 10$ mL, $a = 1$; $V \geq 10$ mL, $a = 2$) (Gatuszka et al., 2012; Yang et al., 2023).

Choline chloride: 0 pictogram + signal word “No” ($0 + 0 = 0$).

Levulinic acid: 1 pictogram + signal word “Warning” ($1 + 1 = 2$).

Ethanol: 2 pictograms + signal word “danger” ($2 + 2 = 4$).

Methanol: 3 pictograms + signal word “danger” ($3 + 2 = 5$).

In this study, the NADES (Ch-Lea) was composed of choline chloride and levulinic acid (molar ratio = 1:2). In the extraction process of flavonoids from *Fructus aurantii*, the amounts of NADES used was 6.00 g (with a water content of 30 %, 1.09 g/cm^3). Thus, the molar concentration of choline chloride was 2.05 mol/L, and the molar concentration of levulinic acid was 4.10 mol/L. In the conventional extraction methods of flavonoids from *Fructus aurantii*, 20 % ethanol (4 mL, 0.97 g/cm^3) and 50 % methanol (10 mL, 0.91 g/cm^3). In the conventional extraction methods of flavonoids from *Fructus aurantii*, 20 % ethanol (4 mL, 0.97 g/cm^3) and 50 % methanol (10 mL, 0.91 g/cm^3) were used, respectively (Wang et al., 2024; Xiao et al., 2020). Thus, the molar concentrations of ethanol and methanol are 3.43 mol/L and 12.35 mol/L, respectively. By calculation, the $PPs_{reagents}$ of NADES (Ch-Lea), methanol, and ethanol were 0.98 points, 12.35 points and 1.39 points, respectively. The results of the $PPs_{instruments}$ of every solvent were shown in Table 1. Due to the

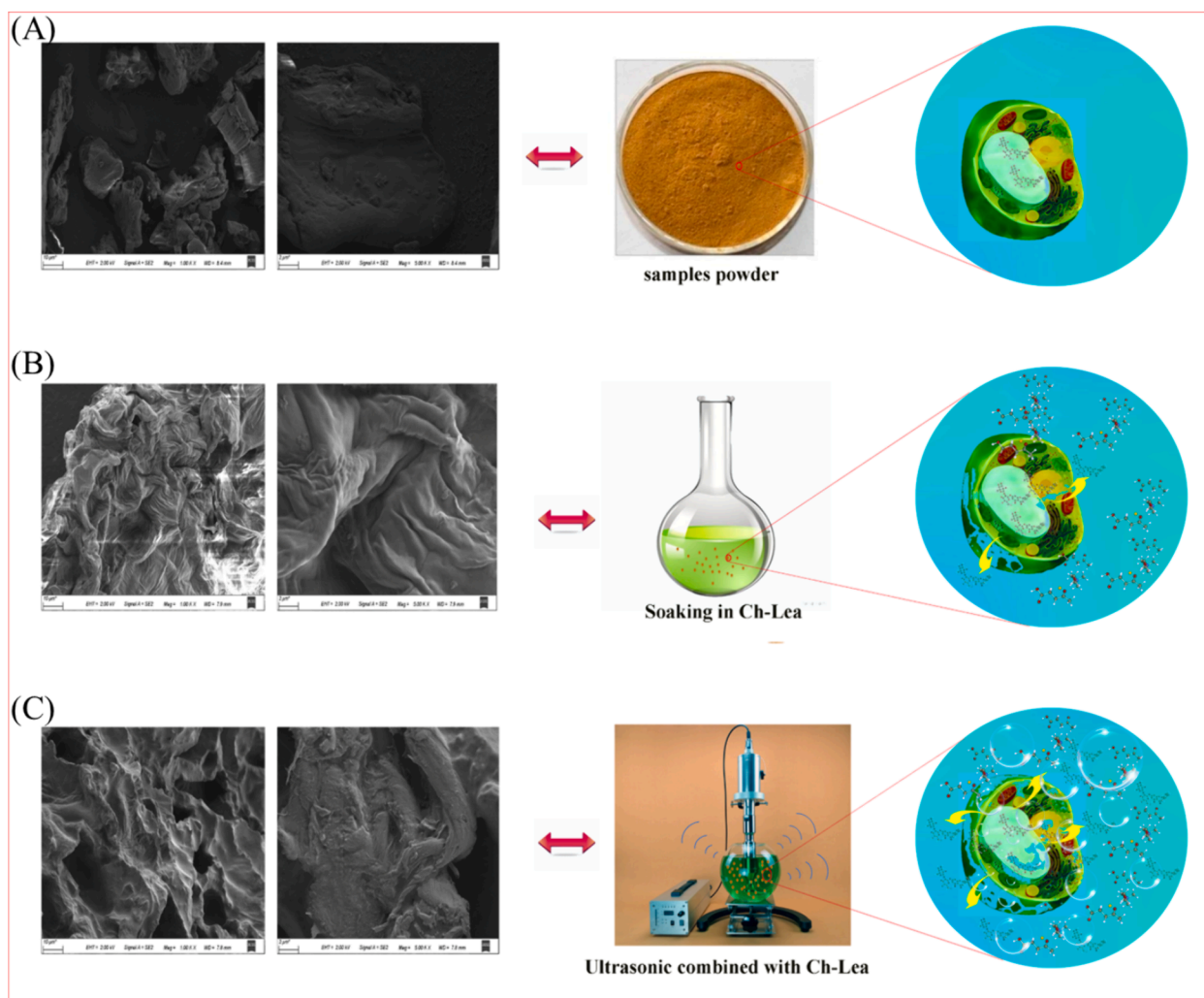


Fig. 8. The SEM microscopic images and cellular structure. (A) Dried *Fructus aurantii* powder, (B) soaking in Ch-Lea, (C) with ultrasonication coupled with Ch-Lea.

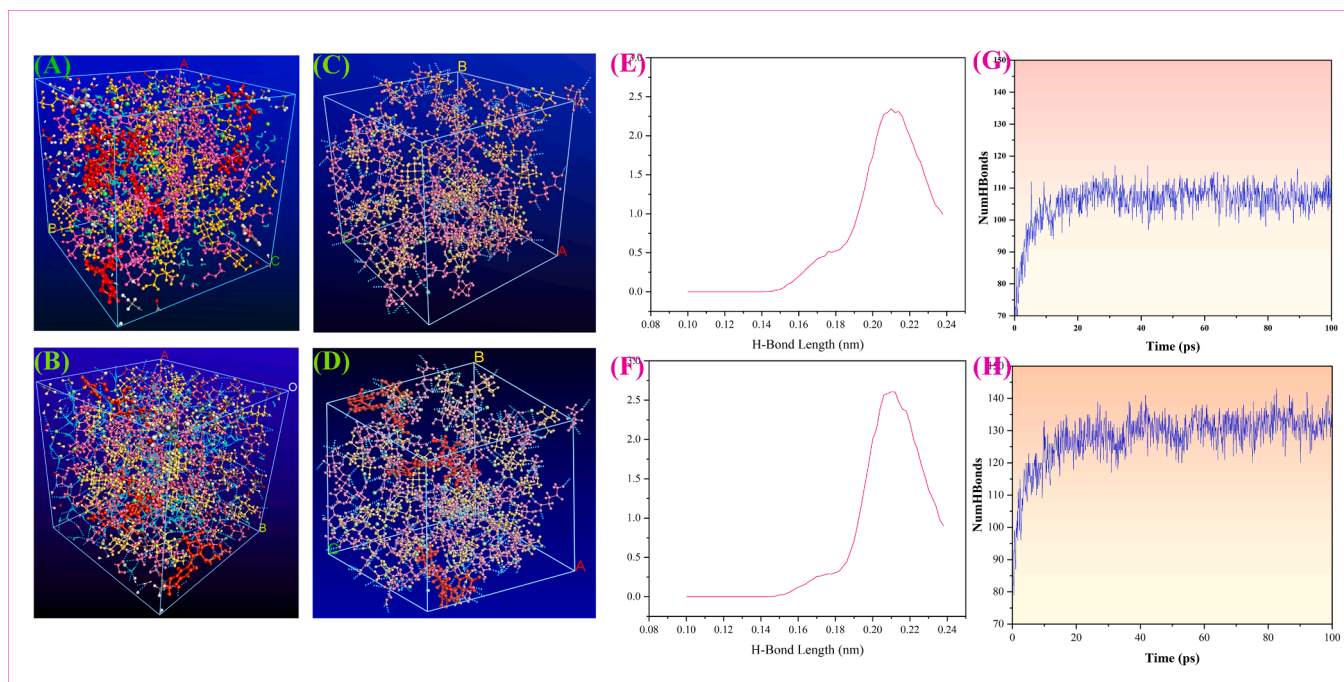


Fig. 9. MD simulation snapshots for configurations. (A) contains naringin, Ch-Lea and water without displaying hydrogen bonds and, (B) contains naringin, Ch-Lea and water with displaying hydrogen bonds. (C) only contains Ch-Lea with displaying hydrogen bonds, (D) contains naringin and Ch-Lea display hydrogen bonds. (E) represents the hydrogen bond length in (C). (F) represents the hydrogen bond length in (D). (G) represents the number of hydrogen bonds in (C), (H) represents the number of hydrogen bonds in (D).

power of all three extraction methods being less than 1.5KWh, the PPs (power) of all three methods were 1 point. Ch-Lea has a non-volatile characteristic, so its PPs (occupational hazard) was 0 points. However, both methanol and ethanol have high volatility and flammability, so the PPs (occupational hazard) of methanol and ethanol was 3 points (Gatuszka et al., 2012; Yang et al., 2023). Ch-Lea had the characteristics of biodegradability or reusability, so the PPs (waste) was 1 point, while the methanol and ethanol cannot be reused, so the PPs (waste) of both methanol and ethanol was 3 points. To sum up, the total score on the Eco-Scale for Ch-Lea extraction was 97.02 points, the total score on the Eco-Scale for ethanol extraction was 91.61 points, and the total score on the Eco-Scale for methanol extraction was 80.65 points. It could be found that the total score on the Eco-Scale of NADES (Ch-Lea) was higher than those of methanol and ethanol.

Based on the above analysis, it can be concluded that NADES (Ch-Lea) was more environmentally friendly and safe compared to traditional extraction solvents.

3.8. Extraction mechanism

3.8.1. Morphological analysis of the residue

In order to further investigate the extraction mechanism of naringin from *Fructus aurantii* by NADES (Ch-Lea), the SEM was utilized for analyzing and comparing the surface morphology of the sample powder and residue before and after extraction. As illustrated in Fig. 8A and Fig. S3, the surface morphology of the raw sample powder is relatively smooth, with intact structure and almost no visible pores or fractures. However, its surface morphology became rough and wrinkled after the sample powder was soaked in Ch-Lea (Fig. 8B), which was due to the influence of Ch-Lea on plant structure erosion and penetration. By comparison, it could be noted that the outer surface of the sample powder showed obvious fracture and loose structure after the synergistic effect of Ch-Lea and pulsed ultrasound (Fig. 8C), which was conducive to the extraction of chemical components.

On the one hand, the NADES has strong penetration and permeability, which could destroy the lignin and cellulose structures of plant

cell walls, resulting in the leakage of intracellular substances into the extracellular space (Zhang et al., 2014). Moreover, the NADES had a strong affinity with the target compound, which could promote the dissolution and extraction of the target component. On the other hand, due to the low vapor pressure characteristics of NADES, the NADES mediated ultrasound can undergo compression and rarefaction cycles, and when the threshold is exceeded, cavitation bubbles are generated (Cao et al., 2019). The implosion or rupture of cavitation bubbles can generate instantaneous high shear force and local turbulence around the bubbles, which leads to the rupture and loosening of plant cell structure, which is the most critical factor (Fu et al., 2020; Fu et al., 2021). Thus, a large amounts of NADES flows into plant cells to extract the target components. In addition, the microflow and nonlinear oscillation of bubbles caused by implosion can effectively mix suspended particles with solvents, break down the barrier of the stagnant layer around the particles, and promote mass transfer and extraction between intracellular components and solvents (Fu et al., 2021). The above-mentioned factors might be the synergistic mechanism of NADES (Ch-Lea) and ultrasound during extraction.

3.8.2. MD and RDG analysis

In order to further explore the extraction aggregation behavior between the target compound and NADES (Ch-Lea), the molecular dynamics simulation (MD) was performed. The MD simulation considered 50 choline chloride molecules, 100 levulinic acid molecules, 2 naringin molecules and 200 water molecules. All structures above were optimized by DFT calculations.

The movement and structure of the naringin molecule and Ch-Lea were shown in Fig. 9A, B. It could be found that the naringin molecule was encompassed by the NADES, the red part was the naringin molecule, the blue part was water, and the other were Ch-Lea. The results showed there is a weak interaction between naringin molecules and Ch-Lea (Pan et al., 2021). The weak interaction was observed through reduced density gradient (RDG) analysis. The results were shown in Fig. 10. The Fig. 10 contains three colors, including blue, red, and green, representing H-bond attraction, van der Waals interaction and repulsion

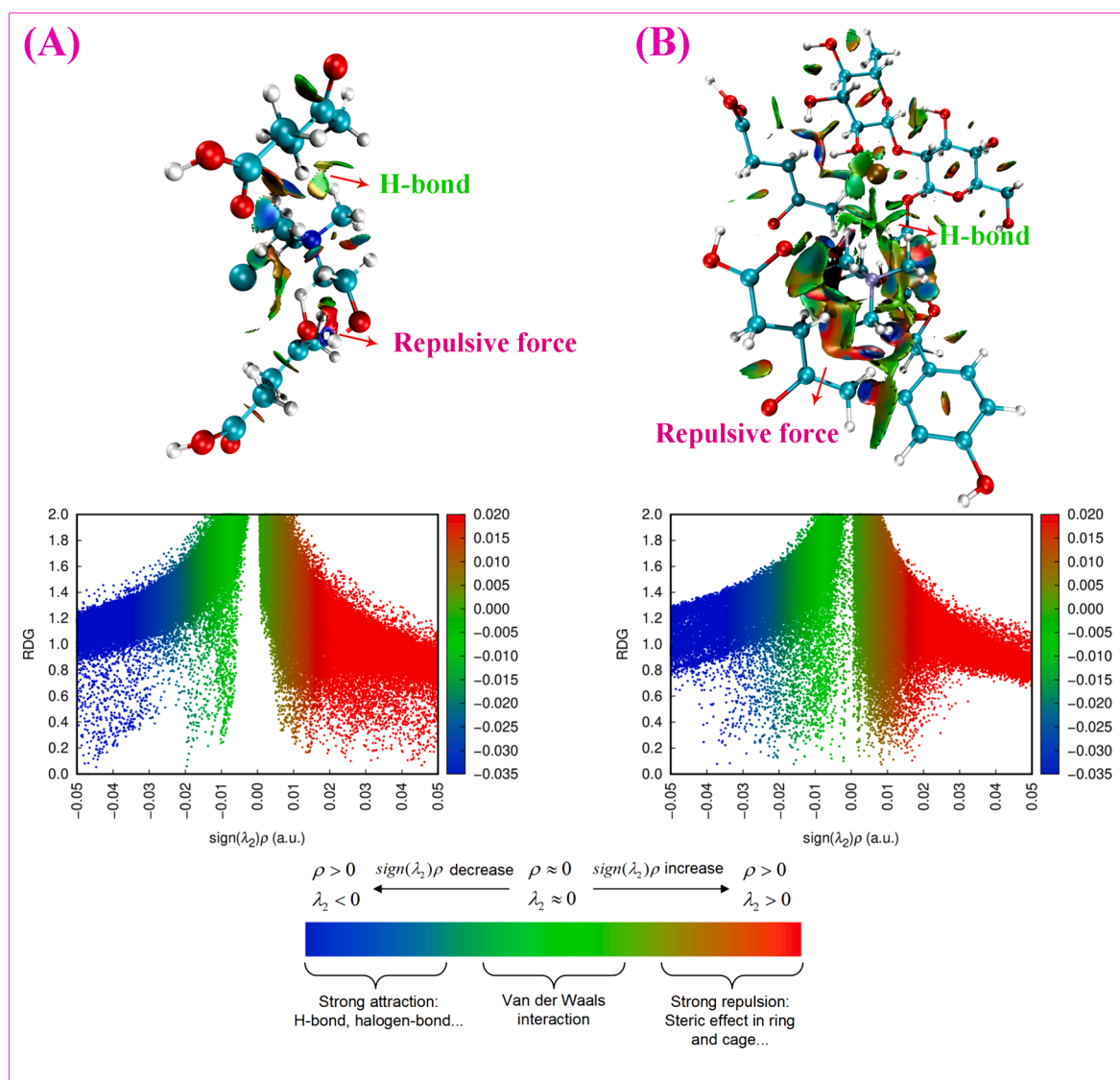


Fig. 10. The 2D and 3D non-covalent interaction plots. (A) Ch-Lea, (B) Ch-Lea and naringin molecules.

between naringin molecules and Ch-Lea, respectively. At the same time, by comparing Fig. 10 A and B, it could be found that the area of the blue part and green in Fig. 10B increases while the red area decreases, indicating that the addition of naringin molecules enhances the hydrogen bonding interactions and van der Waals interaction and weakens the repulsion. The results revealed that the interaction between naringin molecules and Ch-Lea was hydrogen bonding and van der Waals interactions. However, the van der Waals bond interaction strength was very weak, about an order of magnitude lower than the hydrogen bond interaction energy, so the contribution of van der Waals forces in the extraction process of NADES is usually not decisive.

In addition, the number of hydrogen bonds generated by molecular dynamics simulations was statistically analyzed. The results were shown in Fig. 9C, D, G, H. The average number of hydrogen bonds of Ch-Lea was 113, and the number of hydrogen bonds increased to 135 after adding naringin molecules. This result further indicated the generation of a large number of hydrogen bonds between naringin molecules and Ch-Lea. And the Fig. 9E, F showed the bond length of most hydrogen bonds was between 0.14 nm and 0.24 nm, which indicated that the most of hydrogen bonds were strong H-bonds (Xia et al., 2018). It could be concluded that hydrogen bonding interactions were the main driving force for the Ch-Lea extraction of naringin.

The hydrogen bonds mainly originate from O atoms and Cl atoms. The hydrogen bonding interactions of O and Cl atoms were discussed separately in this study for analyzing the hydrogen bonding interactions between Ch-Lea and naringin molecules from an atomic perspective. The results were shown in Fig. 11. The Fig. 11A indicated that the average number of O atoms-H bonds is 15, and the average number of H-bonds has doubled when the naringin molecule was added (Fig. 11B). However, there was no significant change in the number of Cl atoms-H bonds (Fig. 8 11D). The above results implied that the hydrogen bonding interaction between Ch-Lea and naringin molecules mainly contributes to the O atom, while the effect of the chlorine atom could be ignored.

In summary, the hydrogen bonding interactions between the NADES (Ch-Lea) and naringin, especially the O atoms-H bonds, play a predominant role in the naringin extraction process.

4. Conclusion

In the present study, the natural deep eutectic solvents (Ch-Lea), as a new green solvent, was explored for the extraction of flavonoids from *Fructus aurantii*. Firstly, the conductor-like real solvation screening model (COSMO-RS) was employed to screen and design a suitable NADES from eighteen NADES. Then the theoretical analysis (σ -profile,

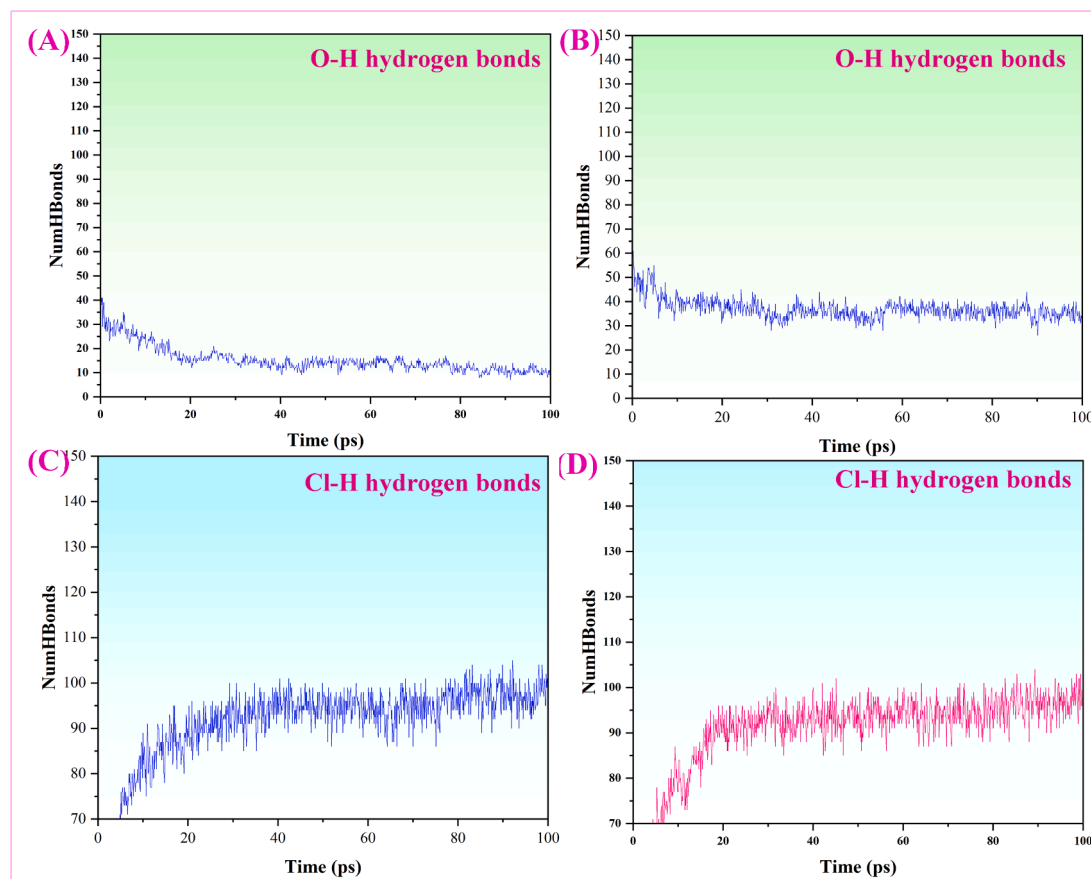


Fig. 11. (A) represents the number of O-H hydrogen bonds of Ch-Lea, (B) represents the number of Cl-H hydrogen bonds of Ch-Lea, (C) represents the number of O-H hydrogen bonds of Ch-Lea and naringin molecules, and (D) represents the number of Cl-H hydrogen bonds of Ch-Lea and naringin molecules.

σ -surface and binding energy) and extraction experiments were used to explain and verify the above screening results. The theoretical and experimental results showed the Ch-Lea was the best extraction solvent. Secondly, the factors affecting extraction efficiency, including the molar ratio, water content, solid/liquid ratio, and extraction time and power, temperature, were screened out. Under the optimal condition, the yield of flavonoids was 122.68 mg/g, which was higher than that of the methanol (115.01 mg/g) and ethanol (112.81 mg/g). Meanwhile, the green assessment of Ch-Lea and traditional extraction solvent (methanol and ethanol) was performed via using Eco-Scale methodology. The results show that Ch-Lea is more efficient and environmentally friendly than traditional solvents. At last, the extraction mechanism was analyzed through molecular dynamics (MD) simulations and reduced density gradient function (RDG) analysis.

5. Author agreement

All Authors declare that this manuscript entitled “Natural deep eutectic solvent-ultrasound for the extraction of flavonoids from *Fructus Aurantii*: Theoretical screening, experimental and mechanism” is original, has not been published before and is not currently being considered for publication elsewhere.

CRediT authorship contribution statement

Hua Du: Data curation, Formal analysis, Funding acquisition, Investigation, Methodology, Project administration, Resources, Software, Validation, Visualization, Writing – original draft, Writing – review & editing. **Wenhui Wu:** Data curation, Formal analysis, Investigation, Methodology, Project administration, Resources,

Software, Validation, Visualization, Writing – original draft, Writing – review & editing. **Yaodeng Wang:** Data curation, Formal analysis, Methodology, Software, Validation, Writing – original draft, Writing – review & editing. **Ping Tang:** Data curation, Formal analysis, Resources, Software, Writing – original draft. **Yi Wu:** Data curation, Formal analysis, Project administration, Software, Writing – original draft. **Jing Qiu:** Investigation, Software, Visualization, Writing – original draft. **Chong Xu:** Data curation, Methodology, Software, Writing – original draft. **Lingzi Li:** Methodology, Software. **Min Yang:** Conceptualization, Formal analysis, Funding acquisition, Project administration, Resources, Supervision, Validation, Visualization, Writing – original draft, Writing – review & editing.

Declaration of competing interest

The authors declare that they have no known competing financial interests or personal relationships that could have appeared to influence the work reported in this paper.

Acknowledgments

This work is supported by Postdoctoral Research Foundation of China (CN): Mechanism of simultaneous extraction of flavonoids and essential oil components from *Fructus aurantii* by the “tailored design” NADES based on quantum chemical calculations (No. 2023 M74043). And Chongqing Science and Technology Bureau: Varieties and quality of *Fructus aurantii* produced in Chongqing (cstc2022ycjh-bgzxm0207).

Appendix A. Supplementary data

Supplementary data to this article can be found online at <https://doi.org/10.1016/j.arabjc.2024.105886>.

References

- Alañón, M.E., Ivanović, M., Gómez-Caravaca, A.M., Arráez-Román, D., Segura-Carretero, A., 2020. Choline chloride derivative-based deep eutectic liquids as novel green alternative solvents for extraction of phenolic compounds from olive leaf. *Arabian Journal of Chemistry* 13 (1), 1685–1701. <https://doi.org/10.1016/j.arabjc.2018.01.003>.
- AlYammahi, J., Darwish, A.S., Almस्ताfa, G., Lemaoui, T., AlNashef, I.M., Hasan, S.W., Banat, F., 2023. Natural deep eutectic solvents for ultrasonic-assisted extraction of nutritious date sugar: molecular screening, Experimental, and prediction. *Ultrasonics Sonochemistry* 98, 106514. <https://doi.org/10.1016/j.ultrsonch.2023.106514>.
- Banjerdpongchai, R., Wudtiwai, B., Khawon, P., 2016. Induction of human hepatocellular carcinoma HepG2 cell apoptosis by naringin. *Asian Pacific Journal of Cancer Prevention* 17 (7), 3289–3294.
- Cao, C., Nian, B., Li, Y., Wu, S., Liu, Y., 2019. Multiple hydrogen-bonding interactions enhance the solubility of starch in natural deep eutectic solvents: molecule and macroscopic scale insights. *Journal of Agricultural and Food Chemistry* 67 (45), 12366–12373. <https://doi.org/10.1021/acs.jafc.9b04503>.
- Chang, X., Lin, S., Wang, G., Shang, C., Wang, Z., Liu, K., Stang, P.J., 2020. Self-assembled perylene bisimide-cored trigonal prism as an electron-deficient host for C(60) and C(70) driven by “like dissolves like”. *Journal of the American Chemical Society* 142 (37), 15950–15960. <https://doi.org/10.1021/jacs.0c06623>.
- Cheng, Y., Zhao, H., Cui, L., Hussain, H., Nadolinik, L., Zhang, Z., Wang, D., 2024. Ultrasonic-assisted extraction of flavonoids from peanut leave and stem using deep eutectic solvents and its molecular mechanism. *Food Chemistry* 434, 137497. <https://doi.org/10.1016/j.foodchem.2023.137497>.
- Cui, Z., Enjome Djocki, A.V., Yao, J., Wu, Q., Zhang, D., Nan, S., Li, C., 2021. COSMO-SAC-supported evaluation of natural deep eutectic solvents for the extraction of tea polyphenols and process optimization. *Journal of Molecular Liquids* 328, 115406. <https://doi.org/10.1016/j.molliq.2021.115406>.
- Dai, Y., Witkamp, G., Verpoorte, R., Choi, Y.H., 2013. Natural Deep Eutectic Solvents as a New Extraction Media for Phenolic Metabolites in *Carthamus tinctorius* L. *Analytical Chemistry* (Washington) 85 (13), 6272–6278. <https://doi.org/10.1021/ac400432p>.
- Della Posta, S., Gallo, V., Gentili, A., Fanali, C., 2022. Strategies for the recovery of bioactive molecules from deep eutectic solvents extracts. *Trends in Analytical Chemistry* (regular Ed.) 157, 116798. <https://doi.org/10.1016/j.trac.2022.116798>.
- Doldolova, K., Bener, M., Lalikoglu, M., Aşçi, Y.S., Arat, R., Apak, R., 2021. Optimization and modeling of microwave-assisted extraction of curcumin and antioxidant compounds from turmeric by using natural deep eutectic solvents. *Food Chemistry* 353, 129337. <https://doi.org/10.1016/j.foodchem.2021.129337>.
- Fu, X., Belwal, T., Cravotto, G., Luo, Z., 2020. Sono-physical and sono-chemical effects of ultrasound: Primary applications in extraction and freezing operations and influence on food components. *Ultrasonics Sonochemistry* 60, 104726. <https://doi.org/10.1016/j.ultrsonch.2019.104726>.
- Fu, X., Wang, D., Belwal, T., Xu, Y., Li, L., Luo, Z., 2021. Sonication-synergistic natural deep eutectic solvent as a green and efficient approach for extraction of phenolic compounds from peels of *Carya cathayensis* Sarg. *Food Chemistry* 355, 129577. <https://doi.org/10.1016/j.foodchem.2021.129577>.
- Gatuszka, A., Migaszewski, Z.M., Koniczka, P., Namieśnik, J., 2012. Analytical Eco-Scale for assessing the greenness of analytical procedures. *Trends in Analytical Chemistry* 37, 61–72. <https://doi.org/10.1016/j.trac.2012.03.013>.
- He, Y., Chen, Y., Shi, Y., Zhao, K., Tan, H., Zeng, J., Xie, H., 2018. Multiresponse optimization of ultrasonic-assisted extraction for aurantii Fructus to obtain high yield of antioxidant flavonoids using a response surface methodology. *Processes* 6 (12), 258. <https://doi.org/10.3390/pr6120258>.
- Hsieh, Y., Li, Y., Pan, Z., Chen, Z., Lu, J., Yuan, J., Zhang, J., 2020. Ultrasonication-assisted synthesis of alcohol-based deep eutectic solvents for extraction of active compounds from ginger. *Ultrasonics Sonochemistry* 63, 104915. <https://doi.org/10.1016/j.ultrsonch.2019.104915>.
- Hu, J., Peng, D., Huang, X., Wang, N., Liu, B., Di, D., Pei, D., 2023. COSMO-SAC and QSPR combined models: A flexible and reliable strategy for screening the extraction efficiency of deep eutectic solvents. *Separation and Purification Technology* 315, 123699. <https://doi.org/10.1016/j.seppur.2023.123699>.
- Jangir, A.K., Lad, B., Dani, U., Shah, N., Kuperkar, K., 2020. In vitro toxicity assessment and enhanced drug solubility profile of green deep eutectic solvent derivatives (DESds) combined with theoretical validation. *RSC Advances* 10 (40), 24063–24072. <https://doi.org/10.1039/c9ra10320a>.
- Khajavian, M., Vatanpour, V., Castro-Munoz, R., Boczkaj, G., 2022. Chitin and derivative chitosan-based structures - preparation strategies aided by deep eutectic solvents: A review. [Journal Article; Review]. *Carbohydr Polym* 275, 118702. <https://doi.org/10.1016/j.carbpol.2021.118702>.
- Khan, H.W., Zailan, A.A., Bhaskar Reddy, A.V., Goto, M., Moniruzzaman, M., 2023. Ionic liquid-based dispersive liquid-liquid microextraction of succinic acid from aqueous streams: COSMO-RS screening and experimental verification. *Environmental Technology ahead-of-print (ahead-of-print)*, 1–12. <https://doi.org/10.1080/09593330.2023.2234669>.
- Klamt, A., Eckert, F., 2003. Erratum to “COSMO-RS: a novel and efficient method for the a priori prediction of thermophysical data of liquids”. *Fluid Phase Equilibria* 205 (2), 357. [https://doi.org/10.1016/S0378-3812\(03\)00097-9](https://doi.org/10.1016/S0378-3812(03)00097-9).
- Lazović, M., Cvijetić, I., Jankov, M., Milojković-Ospenica, D., Trifković, J., Ristivojević, P., 2023. COSMO-RS in prescreening of natural eutectic solvents for phenolic extraction from tucurium chamaedrys. *Journal of Molecular Liquids* 387, 122649. <https://doi.org/10.1016/j.molliq.2023.122649>.
- Lemaoui, T., Darwish, A.S., Hammoudi, N.E.H., Abu Hatab, F., Attoui, A., Alnashef, I.M., Benguerba, Y., 2020. Prediction of electrical conductivity of deep eutectic solvents using COSMO-RS sigma profiles as molecular descriptors: A quantitative structure–property relationship study. *Industrial & Engineering Chemistry Research* 59 (29), 13343–13354. <https://doi.org/10.1021/acs.iecr.0c02542>.
- Li, X., Liang, Q., Sun, Y., Diao, L., Qin, Z., Wang, W., Zarelli, A., 2015. Potential mechanisms responsible for the antineoplastic effects of an aqueous extract of *Fructus aurantii*. *Evidence-Based Complementary and Alternative Medicine* 2015, 491409–491411. <https://doi.org/10.1155/2015/491409>.
- Lu, T., Chen, F., 2012. Multiwfn: a multifunctional wavefunction analyzer. *Journal of Computational Chemistry* 33 (5), 580–592. <https://doi.org/10.1002/jcc.22885>.
- Marsh, K.N., 2006. COSMO-RS from quantum chemistry to fluid phase thermodynamics and drug design. *Journal of Chemical & Engineering Data* 51 (4), 1480. <https://doi.org/10.1021/jc0602317>.
- Mohan, M., Keasling, J.D., Simmons, B.A., Singh, S., 2022. In silico COSMO-RS predictive screening of ionic liquids for the dissolution of plastic. *Green Chemistry: an International Journal and Green Chemistry Resource: GC* 24 (10), 4140–4152. <https://doi.org/10.1039/D1GC03464B>.
- Mushtaq, M., Butt, F.W., Akram, S., Ashraf, R., Ahmed, D., 2022. Deep Eutectic Liquids as Tailorable Extraction Solvents: A Review of opportunities and challenges. *Critical Reviews in Analytical Chemistry* 1–27. <https://doi.org/10.1080/10408347.2022.2125284>.
- Nian, B., Li, X., 2022. Can deep eutectic solvents be the best alternatives to ionic liquids and organic solvents? A perspective in enzyme catalytic reactions. *International Journal of Biological Macromolecules* 217, 255–269. <https://doi.org/10.1016/j.ijbiomac.2022.07.044>.
- Noormohammadi, F., Faraji, M., Pourmohammad, M., 2022. Determination of aromatic amines in environmental water samples by deep eutectic solvent-based dispersive liquid-liquid microextraction followed by HPLC-UV. *Arabian Journal of Chemistry* 15 (6), 103783. <https://doi.org/10.1016/j.arabjc.2022.103783>.
- Pan, H.Y., Wang, Z., Nie, S., Yu, L., Chang, Y., Liu, Z., Fu, Y., 2021. Novel green three-constituent natural deep eutectic solvent enhances biomass extraction from *acanthopanax senticosus* and the extraction mechanism. *ACS Sustainable Chemistry & Engineering* 9 (26), 8835–8847. <https://doi.org/10.1021/acsschemeng.1c02116>.
- Pari, L., Amudha, K., 2011. Hepatoprotective role of naringin on nickel-induced toxicity in male Wistar rats. *European Journal of Pharmacology* 650 (1), 364–370. <https://doi.org/10.1016/j.ejphar.2010.09.068>.
- Qaaid, T., Reza, T., 2023. COSMO-RS predictive screening of type 5 hydrophobic deep eutectic solvents for selective platform chemicals absorption. *Journal of Molecular Liquids* 382, 121918. <https://doi.org/10.1016/j.molliq.2023.121918>.
- Radosević, K., Curko, N., Gaurina Srećek, V., Cvjetko Bubalo, M., Tomašević, M., Kovačević Ganić, K., Radojčić Redovniković, I., 2016. Natural deep eutectic solvents as beneficial extractants for enhancement of plant extracts bioactivity. *LWT* 73, 45–51. <https://doi.org/10.1016/j.lwt.2016.05.037>.
- Sadus, R. J. (2019). Erratum: “Two-body intermolecular potentials from second virial coefficient properties” [J. Chem. Phys. 150, 024503 (2019)]. *Journal of chemical physics* 150(7), 79901. doi: 10.1063/1.5091046.
- Sellaoui, L., Dotto, G.L., Peres, E.C., Benguerba, Y., Lima, É.C., Lamine, A.B., Erto, A., 2017. New insights into the adsorption of crystal violet dye on functionalized multi-walled carbon nanotubes: Experiments, statistical physics and COSMO-RS models application. *Journal of Molecular Liquids* 248, 890–897. <https://doi.org/10.1016/j.molliq.2017.10.124>.
- Wang, R., He, R., Li, Z., Lin, X., Wang, L., 2021. HPLC-Q-Orbitrap-MS/MS phenolic profiles and biological activities of extracts from roxburgh rose (*Rosa roxburghii* Tratt.) leaves. *Arabian Journal of Chemistry* 14 (8), 103257. <https://doi.org/10.1016/j.arabjc.2021.103257>.
- Wang, Y., Wu, W., Li, R., Sun, J., Jiang, G., Yang, M., 2024b. Correlation between active ingredients in *Fructus aurantii* and soil factor. *Chinese Journal of Experimental Traditional Medical Formulae* 30 (03), 133–141.
- Wang, D., Zhang, M., Lim Law, C., Zhang, L., 2024a. Natural deep eutectic solvents for the extraction of lentinan from shiitake mushroom: COSMO-RS screening and ANN-GA optimizing conditions. *Food Chemistry* 430, 136990. <https://doi.org/10.1016/j.foodchem.2023.136990>.
- Xia, Q., Liu, Y., Meng, J., Cheng, W., Chen, W., Liu, S., Yu, H., 2018. Multiple hydrogen bond coordination in three-constituent deep eutectic solvents enhances lignin fractionation from biomass. *Green Chemistry: an International Journal and Green Chemistry Resource: GC* 20 (12), 2711–2721. <https://doi.org/10.1039/C8GC00900G>.
- Xiao, Q., L., Yin, Y., W., Shi, t., W., Xiao, q., Z., Jia, m., T., Jin, W., Yong, M., Z. (2020). Optimization of the extraction process of flavonoids from *Fructus aurantii* by response surface method. *Journal of Hebei North University (Medical Edition)*, 10 (6), 23–26. doi: 10.3969/j.issn.2095-1396.2020.06.004.
- Yang, Y., Ding, Z., Zhong, R., Xia, T., Wang, W., Zhao, H., Shu, Z., 2020. Cardioprotective effects of a *Fructus Aurantii* polysaccharide in isoproterenol-induced myocardial ischemic rats. *International Journal of Biological Macromolecules* 155, 995–1002. <https://doi.org/10.1016/j.ijbiomac.2019.11.063>.
- Yang, D., Qiu, W., Xu, Y., Hu, Z., Wang, L., 2023a. Optimisation and modelling of ultrasonic-assisted extraction of canthaxanthin from *Chromochloris zofingiensis*

- using eutectic solvents. *Industrial Crops and Products* 202, 117002. <https://doi.org/10.1016/j.indcrop.2023.117002>.
- Yang, Z., Yue, S., Gao, H., Zhang, Q., Xu, D., Zhou, J., Tang, Y., 2023b. Natural deep eutectic solvent-ultrasound assisted extraction: A green approach for ellagic acid extraction from *Geum japonicum*. *Frontiers in Nutrition (lausanne)* 9, 1079767. <https://doi.org/10.3389/fnut.2022.1079767>.
- Yu, X., Wang, S., Meng, X., Li, T., Bao, Y., 2017. Simultaneous determination of six components in the flavonoid extract of *Fructus aurantii* by UHPLC. *Journal of Chinese Medicinal Materials* 40 (4), 873–875. <https://doi.org/10.13863/j.issn1001-4454.2017.04.026>.
- Zannou, O., Koca, I., 2020. Optimization and stabilization of the antioxidant properties from Alkanet (*Alkanna tinctoria*) with natural deep eutectic solvents. *Arabian Journal of Chemistry* 13 (8), 6437–6450. <https://doi.org/10.1016/j.arabjc.2020.06.002>.
- Zannou, O., Pashazadeh, H., Ibrahim, S.A., Koca, I., Galanakis, C.M., 2022. Green and highly extraction of phenolic compounds and antioxidant capacity from kinkeliba (*Combretum micranthum* G. Don) by natural deep eutectic solvents (NADESS) using maceration, ultrasound-assisted extraction and homogenate-assisted extraction. *Arabian Journal of Chemistry* 15 (5), 103752. <https://doi.org/10.1016/j.arabjc.2022.103752>.
- Zhang, Y.J., Huang, W., Huang, X., Wang, Y., Wang, Z., Wang, C., Ren, P., 2012. *Fructus aurantii* induced antidepressant effect via its monoaminergic mechanism and prokinetic action in rat. *Phytomedicine* 19 (12), 1101–1107. <https://doi.org/10.1016/j.phymed.2012.05.015>.
- Zhang, H., Wu, S., 2014. Efficient sugar release by acetic acid ethanol-based organosolv pretreatment and enzymatic saccharification. *Journal of Agricultural and Food Chemistry* 62 (48), 11681–11687. <https://doi.org/10.1021/jf503386b>.
- Zhao, J., Zhou, G., Fang, T., Ying, S., Liu, X., 2022. Screening ionic liquids for dissolving hemicellulose by COSMO-RS based on the selective model. *RSC Advances* 12 (26), 16517–16529. <https://doi.org/10.1039/d2ra02001g>.
- Zuo, J., Geng, S., Kong, Y., Ma, P., Fan, Z., Zhang, Y., Dong, A., 2023. Current progress in natural deep eutectic solvents for the extraction of active components from plants. *Critical Reviews in Analytical Chemistry* 53 (1), 177–198. <https://doi.org/10.1080/10408347.2021.1946659>.